

Can one hear the shape of a target zone?

Jean-Louis Arcand^{1*}

Max-Olivier Hongler^{2†}

Shekhar Hari Kumar^{1‡}

Daniele Rinaldo^{1§}

¹The Graduate Institute of International and Development Studies, Geneva

²École Polytechnique Fédérale, Lausanne

Abstract

We develop a target zone model with realistic features such as finite exit time, non-stationary dynamics and heavy tails. Our rigorous characterization of risk corresponds to the dynamic counterpart of a mean-preserving spread. We explicitly solve for both stationary and transient exchange rate paths, and show how they are influenced by the distance to both the time horizon and the target zone bands. This enables us to show how central bank intervention is endogenous to both the distance of the fundamental to the band and the underlying risk. We discuss how the credibility of the target zone is shaped by the set horizon and the degree of underlying risk, and we determine a minimum time at which the required parity can be reached. We prove that the interplay of the diffusive component and the destabilizing risk component can yield an endogenous regime shift characterized by a threshold level of risk above which the target zone ceases to exist. All the previous results cannot obtain by means of the standard Gaussian and affine models. We recover by numerical simulations the different exchange rate densities established by the target zone literature.

JEL Classification: F31,F33, F45, C63

Keywords: Non-stationary exchange rate dynamics; Target Zones; Dynamic mean-preserving spreads; Target Zone Credibility; Spectral Gap; Noise-induced regime shifts.

*jean-louis.arcand@graduateinstitute.ch

†max.hongler@epfl.ch

‡shekhar.hari@graduateinstitute.ch

§daniele.rinaldo@graduateinstitute.ch.

The authors thank Didier Sornette, Ugo Panizza and Cédric Tille for their precious insights.

1 Introduction

The exchange rate target zone literature pioneered by [Krugman \(1991\)](#) is based on a stochastic flexible price monetary model in continuous time. This literature highlights the role of market expectations of fundamentals in shaping exchange rate movements. Given its assumptions of perfect credibility, it implies that central bankers need only intervene marginally at the bounds of the target zone or allow honeymoon effects of credibility to automatically stabilize the exchange rate. The European Monetary System (EMS) and the Exchange Rate Mechanism (ERM), which have existed from 1979 to 1999 until countries adopted the Euro, have provided a natural test bed for this theory.

The target zone model is both well accepted theoretically and has provided the intellectual justification for a nominal anchor for monetary policy. However, there is scant empirical support for the validity of the framework. The U-shaped distribution within the target band and the negative correlation between the exchange rate and the interest rate differential implied by the Krugman model have found little counterpart in the data. In spite of this, the practice of using target zones continued through the 2000's with new member states joining the ERM-II target band and slowly adopting the Euro.¹ For example, Denmark is still in ERM-II with a $\pm 2.5\%$ band with the EUR. It is conceivable that future new member states will go through the ERM process, making target zone modeling of current relevance. Our purpose in this paper is to unpack target zone credibility, while incorporating non-stationary dynamics and heavy tails.

We make three main contributions. First, we model the fundamental dynamics of the exchange rate using the definition of risk which corresponds to Rothschild and Stiglitz's concept of mean-preserving increase in risk. As is well known, risk and variance are not necessarily equivalent, as is commonly assumed in the existing literature. Second, we explicitly consider non-stationary dynamics for a currency to exit a target zone, and show how the credibility of the latter is shaped both by the finite time horizon and the degree of underlying risk. Solving for explicitly time-dependent dynamics also allows us to show how the exchange rate is continuously determined by the distance to the time horizon as well as its distance to the target bands. It turns out that the underlying dynamics are similar to the phenomena famously described by [Kac \(1966\)](#), where he asked whether one could "*hear the shape of a drum*". In the case of exchange rates, in certain situations this can indeed happen, especially when the exchange rate is pushed to the sides of the target band by an additional external force: intuitively, this corresponds to the acoustic difference between striking a tense membrane versus a loose one. This is what we describe in our paper. This allows us to show how the central bank determines its intervention strategies by the degree to which it "feels" the presence of the target zone bounds, and depends critically on the degree of underlying risk and the band size. Third, moving to a theoretically correct definition of risk allows for the emergence of a regime shift once risk reaches a critical threshold, after which the target zone cannot be credibly held.

The standard case of exchange rate dynamics in a finite target zone with Gaussian-driven fundamentals is a simplified, limiting case of our model for which risk and variance are the same, and which fails to provide a palatable explanation for well-known exits such as ERM-I. Correctly specifying risk implies dynamics in which the exchange rate fundamental has a tendency to systematically escape its purely diffusive nature and move away from its expected value. As such, risk can be a destabilizing force which runs counter to the best efforts of a central bank trying to maintain a target zone. This may cause persistent and potentially one-sided deviations from central parity. Moreover, we show that the effect of risk is both nonlinear and discontinuous. For low risk, our dynamics are similar to the standard model. As risk increases, the exchange rate

¹Cyprus, Latvia, Lithuania, Slovenia, Malta, Slovakia, Estonia. The ERM target zone bands in ERM-II is 6.5 times the band size of ERM-I.

process is increasingly destabilized and requires a monotonically increasing minimum time for the target zone to be reached. However, once a critical threshold of risk is crossed, we observe a regime shift in which the minimum time suddenly drops down and the target zone effectively ceases to exist. The intuition behind this result is that the destabilizing portion of the process generated by risk has overwhelmed the diffusive part. This ties directly to the characterization of credibility of a target zone. Credibility corresponds to the central bank being able to reach the set central parity with the agreed bands at the chosen time horizon. Our model shows that considering non-stationary dynamics is paramount in determining whether the chosen horizon is feasible: we characterize the minimum required time necessary for the parity to be reached. Any smaller time horizon chosen by the central bank would not be credible. In contrast, existing models assume away the problem by positing perfect credibility and stationary dynamics. We then show how the model can fit a wide set of scenarios regarding credibility and control, and we recover by Monte Carlo simulations the different exchange rate densities presented by the established target zone literature.

2 Existing literature and motivations

The seminal paper by [Krugman \(1991\)](#) hinges on the assumption of perfect credibility of the target zone, which gives rise to a U-shaped distribution of the exchange rate. This implies that the exchange rate spends most of its time near the bands of the zone, as well as a negative relationship between the interest rate differential and exchange rate volatility. Given this “honeymoon effect”, the central bank only has to intervene marginally at the bands. The only source of risk in this model is the volatility of the Gaussian distribution. The theoretical predictions of the model have been shown not to hold empirically by [Mathieson *et al.* \(1991\)](#), [Meese and Rose \(1991\)](#) and [Svensson \(1991\)](#). This led to the development of so-called second-generation models, which relax Krugman’s assumptions across two dimensions, to allow for imperfect credibility of the target zone and for intramarginal intervention. The first dimension is studied by [Bertola and Caballero \(1992\)](#) and [Bertola and Svensson \(1993\)](#), who relax the notion of credibility and allow for time varying credibility or realignment risk. They show that honeymoon effects disappear when there is a high probability of exchange rate revaluation. Furthermore, [Tristani \(1994\)](#) and [Werner \(1995\)](#) study endogenous realignment risk, as well as including mean-reverting fundamental dynamics.

Allowing for the possibility of realignment is a way of characterizing a riskier fundamental process, motivated by speculative attacks and constant realignment of the ERM currencies. This is achieved by using a diffusion process with jumps, as an *ad-hoc* way of thickening the tails of the distribution in order to better fit the data. The second dimension explored by second-generation models focuses on allowing the fundamental process to be controlled intramarginally, thus generating a hump-shaped distribution where the exchange rate spends most of its time around central parity. [Dumas and Delgado \(1992\)](#) and [Bessec \(2003\)](#), using controlled diffusion processes, show that the honeymoon effects are considerably weakened, putting into question the necessity of a target zone when central banks intervene intramarginally. [Bekaert and Gray \(1998\)](#) and [Lundbergh and Teräsvirta \(2006\)](#) test the implications of the second-generation models, and find mixed evidence with a slight tendency towards the intramarginal interventions hypothesis. [Ajevskis \(2011\)](#) extended the basic target zone model to a finite termination time setting while maintaining the assumptions of the original model: it is the closest to our approach. [Ajevskis \(2015\)](#) extends his earlier contribution by considering the exchange rate to follow a mean-reverting Ornstein-Uhlenbeck (OU) process and compares the difference in exchange rate-fundamental-target zone dynamics between the OU process and a Brownian motion. He solves the stationary problem for the OU process but he is unable to explicitly solve the non-stationary

part of the process.² Recently, [Studer-Suter and Janssen \(2017\)](#) and [Lera and Sornette \(2016, 2018 and 2019\)](#) find empirical evidence for the target zone model for the EUR/CHF floor target zone set by the Swiss National Bank between 2011 and 2015, the latter mapping the Krugman model to the option chain.

In particular, [Lera and Sornette \(2015\)](#) shows how the standard Krugman model can hold in specific cases, such as the EUR/CHF target zone, because of a sustained pressure that continuously pushes the exchange rate closer to the bounds of the target zone, which the central bank tries to counteract. In this particular case, the sustained pressure stemmed from the Swiss Franc being used as a safe asset in the middle of the European crisis. This implies that there is a source of additional risk which is radically different from the diffusive nature of Gaussian noise. This risk destabilises the exchange rate fundamentals and creates an extra tendency to escape from its mean and move towards the boundary. [Rey \(2015\)](#) famously argued that the global financial cycles stemming from the United States generates additional risk for central banks targeting a nominal anchor. Additionally, [Gopinath and Stein \(2019\)](#) and [Kalemli-Özcan \(2019\)](#) show how US monetary policy shocks can affect the exchange rate of a country with minimal USD exposure because of the dominant nature of the USD as a trade currency. All of these examples represent possible sources of external risk that need to be included in the modeling of the fundamental process. All pre-existing attempts at modeling fundamental risk involve either the variance of Gaussian noise or the addition of ad-hoc jumps.

That risk and variance do not necessarily coincide is often forgotten in applied economic research.³

Specific dynamics or phenomena cannot be represented by conflating all available information on risk solely on the variance parameter of the Gaussian distribution. We therefore adopt a definition of risk which corresponds to the concept of a mean-preserving increase in risk, in the form of second-order stochastic dominance, often referred to as a mean-preserving spread. This concept has been introduced in a static setting by the fundamental works of [Rothschild and Stiglitz \(1970 and 1971\)](#), who define two sufficient integral conditions that allow one to unambiguously rank distributions in terms of their riskiness. This concept has been extended to a dynamic setting by [Arcand *et al.* \(2019\)](#): the authors prove that, among diffusion processes, the *only* process with nonlinear drift and a Brownian bridge satisfying the dynamic equivalent of the two integral conditions is the *Dynamic Mean-Preserving Spread* process (DMPS), which is a non-Gaussian process with a hyperbolic function as drift. The parameter that modulates the nonlinear drift determines the risk of the process, as well as controlling the weight of the tails of its distribution. This process allows one to rigorously characterize the risk of a stochastic process while both escaping the Gaussian straightjacket, allowing for heavier tails, and maintaining analytical tractability. This also allows us to precisely characterize the interplay of diffusive and

²We provide the full solution of the mean-reverting OU case in Appendix C, as a further contribution of this paper.

³As a descriptive example, consider two lotteries x_1 and x_2 , each given by:

$$\begin{aligned} x_1 &= [(0.01, 0.10); (0.10, 0.00); (1, 0.70); (10, 0.00); (100, 0.20); (1090, 0.00)], \\ x_2 &= [(0.01, 0.00); (0.10, 0.01); (1, 0.00); (10, 0.98); (100, 0.00); (1090, 0.01)], \end{aligned}$$

where each pair (x_{ij}, p_{ij}) corresponds to the probability p_{ij} of the realization x_{ij} , for lottery $j = 1, 2$ and states of nature $i = 1, 2, 3, 4, 5, 6$. Notice that the expected values of the two lotteries are the same: $\mathbb{E}x_1 = \mathbb{E}x_2 = 20.701$. However, $\text{Var } x_1 = 2,000.7 < 11,979 = \text{Var } x_2$. Despite the variance of x_2 being much larger than the variance of x_1 , an agent with logarithmic utility will strictly prefer x_2 over x_1 because $\mathbb{E} \log x_1 = 0.46 < 2.303 = \mathbb{E} \log x_2$. The two lotteries cannot unambiguously be ranked in terms of their risk, while they can be in terms of their variance. This simple example illustrates the reason why we want to introduce in our model a rigorous characterization of risk.

ballistic forces⁴: the tendency of external risk to push the exchange rate towards the bounds of the zone is counteracted by the central bank's efforts to maintain the fundamental fluctuating around its mean. This is precisely what is argued by [Lera and Sornette \(2015\)](#). The standard Gaussian case is a limiting case for which the risk parameter is zero. This is a more realistic characterization of fundamental risk, especially considering the influx of external risk given by global financial cycles. We show how the solution of the model consists in the sum of two equations. The first is the time-independent stationary part, which corresponds to the behavior of the exchange rate at the time of entry in the target zone, and the second is the transient part, which describes the sensitivity of the exchange rate to the distance to the bands, as a function of risk, band size and time to exit.

The paper is organised as follows. In Section 3 we extend the traditional stationary framework in order to include non-stationary dynamics, modeling the risk of the fundamental process by means of dynamic mean-preserving spreads. Section 4 discusses the connection between risk, target zone width and credibility. In Section 5 we show the emergence of regime shifts once a critical threshold of risk is reached. Section 6 explains the numerical methods employed in the model simulations, and presents the results. Section 7 discusses possible interpretations and sources of external risk, while section 8 concludes and discusses an agenda for future research.

3 Target zone exit with a finite time horizon

Our starting point is the exchange rate equation given by:

$$X_t = r f_t + \frac{(1-r)}{\alpha} \mathbb{E} \left\{ \frac{dX_t}{dt} \right\}, \quad r \in [0, 1], \quad (1)$$

where f_t describes the dynamics of the logarithm of a fundamental, the stochastic process dW_t is the standard White Gaussian Noise (WGN), X_t stands for the logarithm of the exchange rate at time t and $\mathbb{E} \{dX_t\}$ describes a forward-looking estimation of the logarithm of the exchange rate. The parameter $\alpha > 0$ with the dimension of a frequency (i.e. 1/[time unit]) modulates the size of the forward-looking time window. The ratio $r \in [0, 1]$ weights the relative importance attributed to the present fundamental position versus its forecasted estimate.

As stated before, we want to model the risk of the fundamental in order to include a more rigorous characterization of risk, allowing for non-Gaussianity and heavier tails, yet allowing analytical tractability. We choose as a process for $f(t)$ the dynamic mean-preserving spread (DMPS) process, defined as

$$df_t = \lambda \tanh(\lambda f_t) dt + dW_t, \quad f_{t=0} = f_0, \quad (2)$$

where the nonlinear drift $\lambda \tanh(\lambda f_t)$, $\lambda \in \mathbb{R}^+$ generates a probability spread (an increase in risk) around the mean of the fundamental. The process (2) is a non-Gaussian process that allows to modulate the risk of the fundamental by means of the parameter λ and control the weight of the tails of its distribution⁵. We can allow for a rescaling of the log-fundamental process by a sensitivity parameter $\sigma < 1$, and equation (2) can easily be written as

⁴By ballistic forces we mean a drift component leading to a variance that is increasing quadratically in time

⁵We note yet again that an increase in risk via a DMPS noise source is not the same as just an increase in variance: a situation where the fundamental is driven simply by Gaussian fluctuations around a mean is discussed in detail in [Appendix C](#).

$$df_t = \beta \tanh(\beta f_t) dt + \sigma dW_t, \quad (3)$$

where $\beta = \lambda\sigma$ is the rescaled risk parameter. We allow explicitly time-dependent dynamics $X_t = X(t, f_t)$, and therefore study non-stationary behavior. For $f_0 = 0$, the fundamental dynamics do not affect the systematic vanishing average of f_t , but the repulsive drift $\beta \tanh(\beta f)$ introduces an extra tendency (risk) to escape from $f = 0$. The analysis of the case of mean-reverting fundamentals is presented in Appendices D and E, where we fully solve both Ornstein-Uhlenbeck (O-U) and non-Gaussian, softly attractive dynamics. The latter can be of interest for researchers as an alternative to the O-U process, since it allows to escape Gaussianity and to model an ergodic process with light attraction towards its long-run level, whilst remaining fully analytically tractable.

Using Itô calculus, Eq.(1) rewrites as :

$$\partial_t X(t, f) + \frac{\sigma^2}{2} \partial_{ff} X(t, f) + \beta \tanh(\beta f) \partial_f X(t, f) - \frac{\alpha}{(1-r)} X(t, f) = -\frac{r\alpha}{(1-r)} f. \quad (4)$$

Note the presence of the additional term $\partial_t X(f)$ in Eq.(4) which does not appear when one focuses only on stationary situations. The solution of (4) can be written as the sum of the time-independent stationary solution and the transient solution, i.e.

$$X(\tau, f) = X^*(\tau, f) + X_S(f). \quad (5)$$

Appendix A shows how the stationary solution of (5) is given by

$$X_S(f) = \frac{1}{\cosh(\beta f)} \{A\mathcal{Y}_1(f) + B\mathcal{Y}_2(f) + Y_P(f)\}, \quad (6)$$

where we have

$$\begin{cases} \mathcal{Y}_1(f) = \exp \left\{ +\sqrt{\left[\beta^2 + \frac{2\alpha}{(1-r)\sigma^2}\right]} f \right\}, \\ \mathcal{Y}_2(f) = \exp \left\{ -\sqrt{\left[\beta^2 + \frac{2\alpha}{(1-r)\sigma^2}\right]} f \right\}, \\ Y_P(f) = \frac{2\alpha r (f(2\alpha + \beta^2(1-r)(1-\sigma^2)) \cosh(\beta f) + 2(1-r)\beta\sigma^2 \sinh(\beta f))}{(2\alpha + \beta^2(1-r)(1-\sigma^2))^2} \end{cases} \quad (7)$$

In Eqs. (6) and (7) the couple of constants A and B can be determined by smooth fitting at the bounds $\underline{f} = -\bar{f}$,⁶:

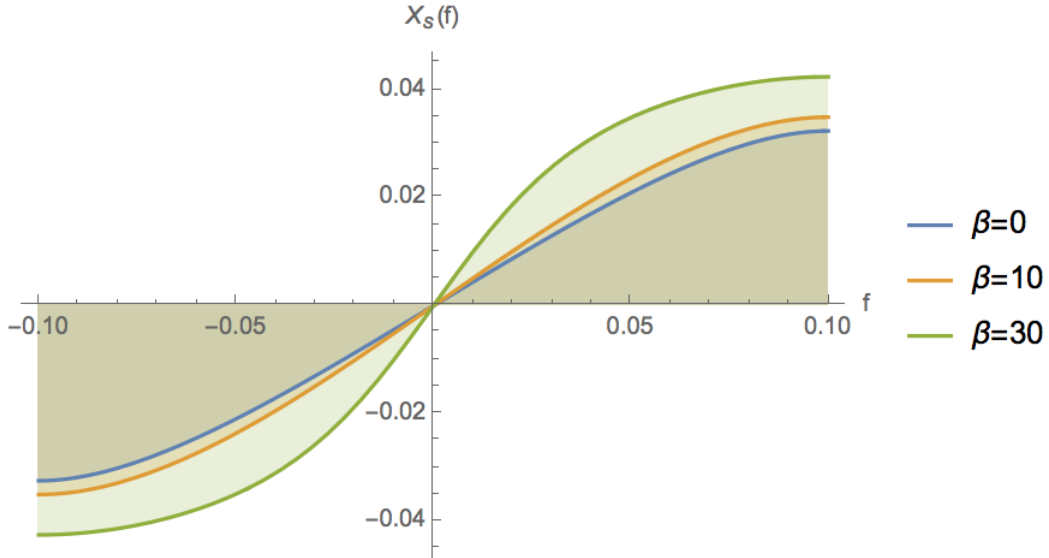
$$\partial_f X_S(f) |_{f=\underline{f}} = \partial_f X_S(f) |_{f=\bar{f}} = 0. \quad (8)$$

The two constants of integration A and B can be obtained in closed form but their expression is lengthy and therefore omitted. An illustration of the stationary solution (6) is presented in Figure 1, which also shows how an increase in the riskiness β of the fundamental prompts the (stationary) exchange rate to behave more independently of the dynamics of the fundamental. At high levels of β , the exchange rate dynamics are driven mostly by the risk and depend less

⁶For simplicity we focus our attention to targets zones symmetric with respect to $f = 0$, although the results hold for general bounds.

on fundamentals, especially around the bounds, as represented by the steepening of the central slope. In this figure, $\bar{f} = 10\%$ and we assume a quasi-daily time step for the expectation $dt = 1/200$ with $r = 0.5$ which implies an equal weight on the fundamental position versus its forecasted estimate. These are important assumptions for our setup. We know that fundamental macroeconomic forecasts do poorly at forecasting the exchange rate at horizons over one year. The violation of uncovered interest parity is a well established fact. This could be because of an exchange rate premium (country/liquidity risk) or due to expectations being biased in finite samples. [Evans and Lyons \(2002\)](#) and [Evans \(2010\)](#) use a portfolio shift model to account for market microstructure pressures by adding order flows as a predictor and they find that it improves the predictability of the exchange rate. This model is useful at higher frequencies where there is an immediate impact on order flow pressures on prices. They argue that order flow reveals advance information about future fundamentals or private information about risk premia. [Chinn and Moore \(2011\)](#) and [Ferreira et al. \(2019\)](#) also make the case that expectation errors of exchange rate using fundamentals are systematic and they show that a hybrid approach of using order flows as a proxy for these expectation errors significantly improves the exchange rate predictions. We believe our parametrization of $dt = 1/200$ with $r = 0.5$ corresponds to a case of fast agent updating with equal weight on fundamentals is similar to the case of [Ferreira et al. \(2019\)](#) and [Coibion and Gorodnichenko \(2015\)](#). Changing the dt to a more fundamental updating frequency, $dt = 1/12$ for example, will reduce the sensitivity of the exchange rate to the fundamentals. Moreover, changing the $r > 0.5$ will increase the sensitivity of the exchange rate to fundamental process.

Figure 1 Effect of varying β on exchange rate dynamics



We now turn to the transient dynamics. At a given time horizon $t = T$, we fix the predetermined exchange rate $X(T, f) = 0$. In terms of the backward time $\tau = T - t$, we write the transformation $X^*(\tau, f) = Y^*(\tau, f) / \cosh(\beta f)$. The time-dependent partial differential equation we need to solve is therefore given by

$$\partial_\tau Y^*(\tau, f) - \frac{\sigma^2}{2} \partial_{ff} Y^*(\tau, f) + \left[\frac{\beta^2}{2} + \frac{\alpha}{(1-r)} \right] Y^*(\tau, f) = 0. \quad (9)$$

with boundary conditions given by

$$\begin{cases} [\partial_f Y^*(\tau, f) - \beta \tanh(\beta f) Y^*(\tau, f)]_{f=\underline{f}} = 0, \\ [\partial_f Y^*(\tau, f) - \beta \tanh(\beta f) Y^*(\tau, f)]_{f=\bar{f}} = 0. \end{cases} \quad (10)$$

We express the solution $Y(\tau, f)$ as $Y^*(\tau, f) = \phi(\tau)\psi(f)$, and proceed to solve this equation by separation of variables and expansion over the basis of a complete set of orthogonal eigenfunctions. Sturm-Liouville theory allows us to state that on the interval $[-\bar{f}, +\bar{f}]$, one has a complete set of orthogonal eigenfunctions $\psi_k(f)$ satisfying Eq.(8), namely:

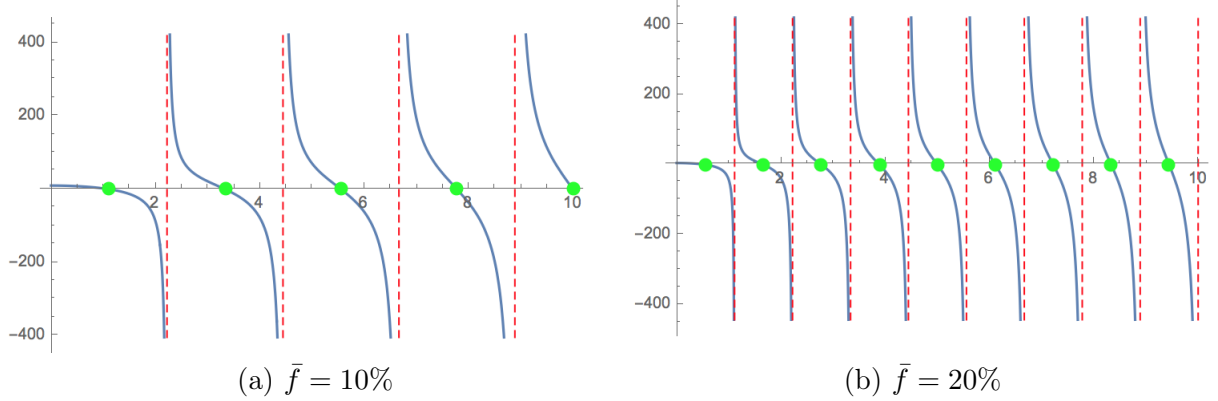
$$\psi_k(f) = \sin\left(\frac{\sqrt{2}\Omega_k}{\sigma} f\right) \quad \in [\underline{f}, \bar{f}], k = \mathbb{N}^+, \quad (11)$$

where each eigenvalue Ω_k solves the transcendental equation

$$\frac{\sqrt{2}\Omega_k}{\sigma} \cot\left(\frac{\sqrt{2}\Omega_k}{\sigma} \bar{f}\right) = \beta \tanh(\beta \bar{f}).$$

Figure 2 Target band and spectrum

Graphical illustration of the solution of equation (3), showing the effect of varying \bar{f} on the spectrum Ω_k .



Furthermore, the eigenvalues are real and span a discrete spectrum:

$$\{\Omega_k\} := \{\Omega_k(\beta, \bar{f})\}, \quad k \in \mathbb{N}^+.$$

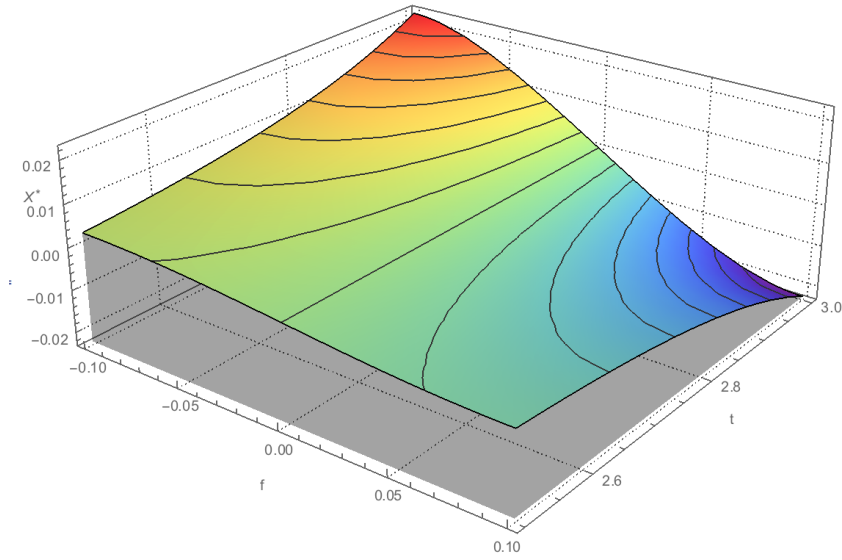
and can therefore be ordered as

$$\Omega_1(\beta, \bar{f}) < \Omega_2(\beta, \bar{f}) < \dots$$

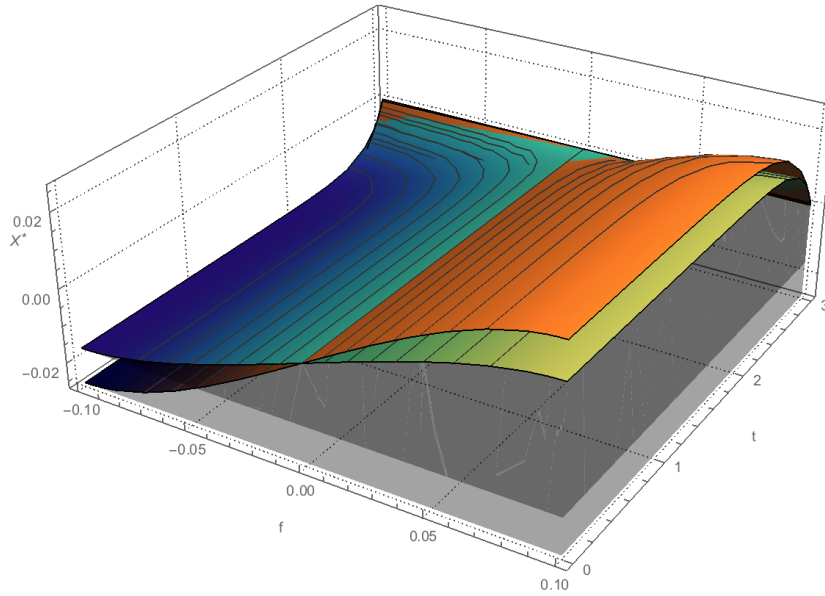
For any $k \in \mathbb{N}^+$, the corresponding $\Omega_k(\beta, \bar{f})$ solves the transcendental equation (3), and has to be calculated numerically. For a general $\beta > 0$, one observes that the successive eigenvalues are not evenly spaced with a distance decreasing with k . The spectrum is controlled by the width of the target zone \bar{f} : the wider is the band, the smaller the separation. The spectrum and its relationship with the target band size are illustrated in Figure 5. Observe also that in the limit $\beta = 0$, one straightforwardly verifies that from Eq.(11) one obtains the evenly spaced set $\Omega_k(0, \bar{f}) = (2k + 1)\frac{\pi}{2\bar{f}}$.

Figure 3 Transient dynamics

Note: This figure shows the evolution of $X(T-t, f)$ of the transient dynamics in the target zone. In Panel (A), we assume a target zone which has been set $T = 3$ years, with $\beta = 1$ for a given set of fundamentals. For the sake of brevity we truncate the figure towards the end of the target zone to effectively illustrate the transient dynamics. In Panel (B) we illustrate the difference in transient dynamics for different β values. Here we have assumed a target band symmetric around zero, i.e. $\bar{f} = 10\% = -\underline{f}$. We also assume $r = 0.5, \alpha = 20$. We truncate the eigenfunction expansion at 50. The second panel illustrates the change in dynamics from $\beta = 0$ (Gaussian) to $\beta = 5$.



(A)



(B)

The development of the transient solution $X^*(\tau, f)$ over the complete set $\{\psi_k(f)\}$ enables one to finally write the full expansion in the following way:

$$\begin{aligned}
X^*(\tau, f) &= X^*(T - t, f), \quad t \in [0, T] \\
&= \frac{1}{\cosh(\beta f)} \sum_{k=1}^{\infty} c_k \exp [-(\Omega_k^2 + \rho)(T - t)] \sin \left[\frac{\sqrt{2}\Omega_k}{\sigma} f \right] \\
c_k &= -\frac{1}{f} \int_{-\bar{f}}^{+\bar{f}} X_S(f) \sin \left[\frac{\sqrt{2}\Omega_k}{\sigma} f \right] df \\
\rho &= \left[\frac{\beta^2}{2} + \frac{\alpha}{(1 - r)} \right].
\end{aligned} \tag{12}$$

The full derivation is reported in Appendix A. When $t = T$, from Eq.(13), by construction of the Fourier coefficients c_k , we have $X^*(0, f) = -X_S(f)$ and so $X(T, f) = X^*(0, f) + X_S(f) = 0$ thus reaching the required fixed parity. An illustration of the transient exchange rate dynamics, as well as the overall transition dynamics throughout the time interval $[0, T]$, is presented in Figure 3. This solution allows to express the movements of the exchange rate via a weighted sum of its stationary behavior, its distance to the exit time and the distance between its value at any time t and the target band. The eigenvalues modulate the frequency of both fundamental and exchange rate movements within the band. The Fourier coefficients c_k represent the impact of the size of the target band in the overall dynamics, via their weight on the infinite series of frequency components (the “harmonics” of the exchange rate path). Loosely speaking, this formulation of the solution allows one to describe the sensitivity of the exchange rate to the distance to the target band. Once the eigenvalues and the eigenfunctions are known, as famously asked by Kac (1966), “if one had perfect pitch”, one would be able to “hear” the shape of the target zone⁷.

This formulation of the solution allows us to uncover the unique nature of the smooth-pasting conditions: the exchange rate process is not reflected at the bounds in the probabilistic sense, since this would have been modeled as a zero derivative condition on the transition probability density function. We are in the presence of “soft” boundaries, where the central bank interventions are determined by the interplay of the distance of the exchange rate to the bounds as well as the tendency of the fundamental to hit them (the risk): this is what is implied by the eigenfunction expansion of the solution. This allows us to “endogenize” the bands: because of the presence of expectations in the exchange rate equation (4), we have a second-order term which allows us to solve the equation in its Sturm-Liouville form and eigenfunction expansion. The Fourier coefficients modulate the sensitivity of the exchange rate to the distance to the band, allowing for the central bank to intervene whenever the fundamental is “felt” to be approaching the bounds. This “feeling” is in fact a direct translation of how much the fundamental tends to escape and how much the central bank needs to intervene marginally or intramarginally: this is a direct consequence of the presence of expectations in the exchange rate equation. In other words, the higher the tendency to hit the bounds and the greater is the likelihood that the central bank will actually intervene intramarginally, with increasingly less regard towards the actual position of the fundamental within the band. One can therefore see that the higher is the risk (the fundamental’s tendency to escape from its central position), the more will the

⁷Note that the time-independent part of the problem is a one-dimensional Neumann problem on the boundary $\partial D = [f, \bar{f}]$

$$\begin{cases} \Delta f + \Omega f = 0 \\ \nabla f|_{\partial D} = 0, \end{cases}$$

which is exactly the problem of finding the overtones on a vibrating surface.

central bank intervene intramarginally. The same applies when the target band shrinks. The standard Krugman framework applies when the fundamental is a pure Brownian motion and the central bank only intervenes marginally. Note that this phenomenon is directly a consequence of our rigorous characterization of fundamental risk. In Section 6 we show how the model can replicate the different exchange rate densities under different assumptions of credibility and intervention⁸. We also point out that this framework potentially allows for the existence of *de jure* and *de facto* bands, as noted by Lundbergh and Teräsvirta (2006): if the *de jure* band is large, expectations over the magnitude of risk may react to a narrower *de facto* band. This is a phenomenon commonly observed in most ERM countries.

4 Risk, target width and credibility: the role of the spectral gap

Here we discuss the interplay between the risk parameter β , the size of the target band $[-\bar{f}, +\bar{f}]$ and the credibility of the time horizon T at which to reach the target zone. We first note that at the initial time $t = 0$, from Eq.(13) we have $X^*(T, f) \approx 0$ and therefore $X(0, f) = X^*(T, f) + X_S(f) \approx X_S(f)$. Since $\Omega_1(\beta, \bar{f}) < \Omega_2(\beta, \bar{f}) < \dots$, one can approximately write:

$$X(T, f) \simeq X_S(f) + \mathcal{O}\left(e^{-(\Omega_1^2 + \rho)T}\right).$$

While for the exact solution we should have $X(T, f) = X_S(f)$, one sees immediately that $X(T - t, f) = X_S(f) + X^*(T - t, f)$ with $X^*(T - t, f)$ given by Eq.(13) nearly matches the exact solution provided we have an horizon interval $T \gtrsim t_{\text{relax}}$ where $t_{\text{relax}} := (\Omega_1^2 + \rho)^{-1}$ is the characteristic relaxation time of the exchange rate process. This provides therefore a validity range for the transient dynamics given by the expansion Eq.(13).

Hence, at time $t = 0$, the required initial probability $X_S(f)$ law is reached only for a large enough time horizon $T \gtrsim t_{\text{relax}}$. This now enables us to link the transient dynamics of $X^*(t, f)$ to the **credibility** of the target zone: the relaxation time τ_{relax} determines the *minimum time interval* for which a credible target zone may be maintained. The larger β (the risk of the fundamental), the greater is the tendency of the fundamental to escape from its mean; the authorities need therefore to maintain the target zone for a longer minimum duration. An increase in risk, for a given \bar{f} , implies that the target zone would have to be set for a longer horizon T to be credible. Alternatively, for a given risk β , an increase of the target zone width \bar{f} , requires a longer minimal T implementation to ensure the overall credibility of the policy. In other words, the central bank has to impose that the time horizon T is at least as large as the relaxation time t_{relax} .

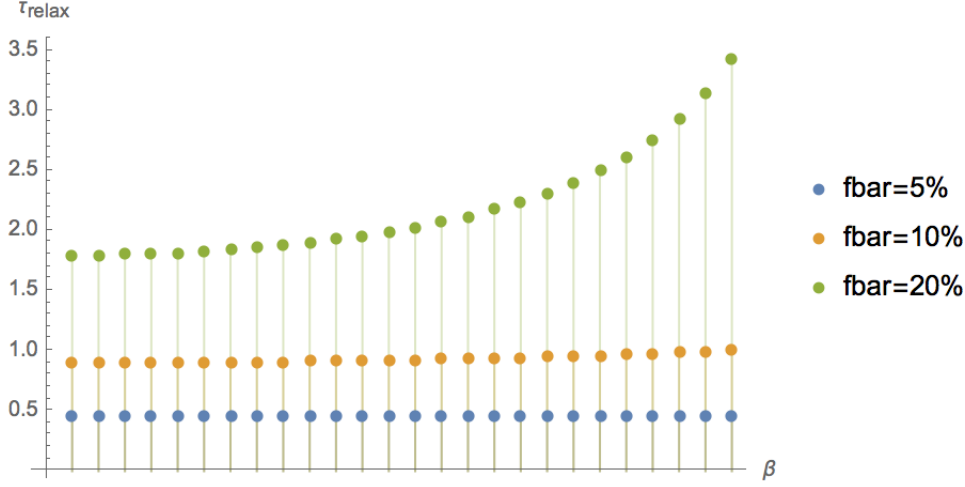
An intuitive interpretation of the relaxation time in this framework is to understand t_{relax} as the characteristic elapsed time required to “feel” the first effects of the home central bank’s actions aimed at reducing fluctuations of the exchange rate, compared to a free float. The bank’s actions may be then viewed as a *de facto* reduction of the target zone band over time, whilst the *de jure* band remains unchanged. A possible implication would be that t_{relax} would be the minimum time for agents to update their priors accurately, generating self-fulfilling expectations that create the honeymoon effect.

The inverse of the relaxation time is determined by the **spectral gap**, which is the distance between 0 and the smallest eigenvalue. We therefore have the relationship $(t_{\text{relax}})^{-1} = (\Omega_1^2 + \rho)$. The spectral gap controls the asymptotic time behaviour of the expansion given by (13), and it is continuously dependent on risk β and band \bar{f} . This relationship is illustrated in Figure 4.

⁸For additional information, see Figure 2 in Crespo-Cuaresma *et al.* (2005)

Figure 4 Interaction between β and \bar{f}

Note: This figure shows the interaction of varying risk (β) and varying the band size (\bar{f}). An increase in risk, for a given \bar{f} , implies that the lowest eigenvalue Ω_1 falls (Panel (A)). The inverse of this value controls the t_{relax} .



Let us now study analytically the behaviour of the solution Ω_1 of the transcendent Eq.(3). Writing $z = \sqrt{2}\Omega_1\bar{f}$, Eq.(3) implies that the product $\beta\bar{f}$ is the determinant of the amplitude of Ω_1 . An elementary graphic analysis enables to conclude that two limiting situations can be reached:

$$\begin{cases} \beta\bar{f} \ll 1 & \Rightarrow & z \lesssim \frac{\pi}{2} & \Rightarrow & \Omega_1 \lesssim \frac{\pi}{2\bar{f}} & \Rightarrow & t_{\text{relax}}^{-1} \lesssim \left[\frac{\pi}{2\bar{f}}\right]^2 + \frac{\beta^2}{2} + \frac{\alpha}{(1-r)}, \\ \beta\bar{f} \gg 1 & \Rightarrow & z \gtrsim \pi & \Rightarrow & \Omega_1 \gtrsim \frac{\pi}{\bar{f}} & \Rightarrow & t_{\text{relax}}^{-1} \gtrsim \left[\frac{\pi}{\bar{f}}\right]^2 + \frac{\beta^2}{2} + \frac{\alpha}{(1-r)}. \end{cases}$$

and therefore:

$$\frac{1}{\left[\frac{\pi}{\bar{f}}\right]^2 + \frac{\beta^2}{2} + \frac{\alpha}{(1-r)}} \leq t_{\text{relax}} \leq \frac{1}{\left[\frac{\pi}{2\bar{f}}\right]^2 + \frac{\beta^2}{2} + \frac{\alpha}{(1-r)}}. \quad (13)$$

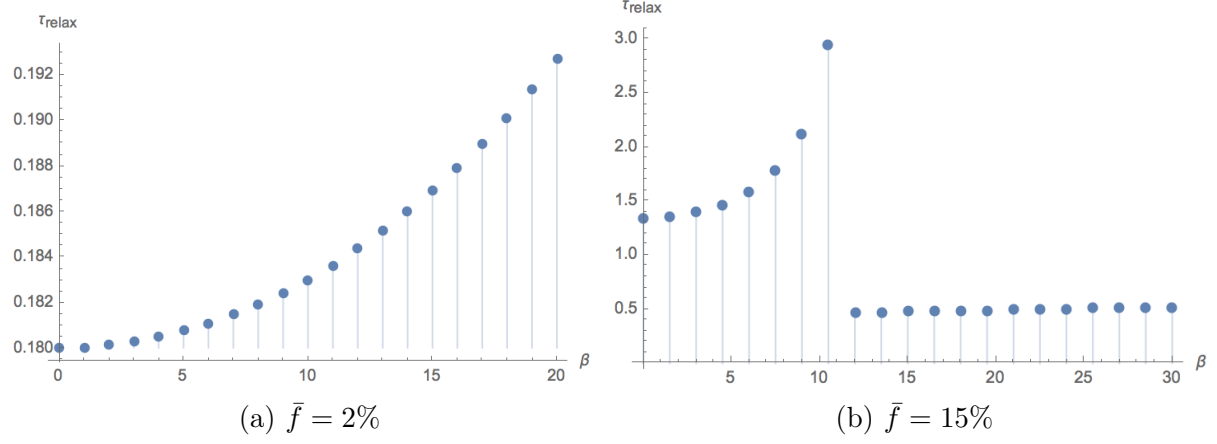
Eq.(13) together with Figure 4, exhibits how an increase in risk β affects t_{relax} more strongly when the exchange rate is allowed to float in a wider band width \bar{f} .

5 Risk, target band and regime shifts

An unique phenomenon that emerges when considering repulsive drifts, and in particular our specification, is the emergence of a *regime shift*. Figure 5(b) shows that for a large enough target band, after a threshold level in β , the relaxation time suddenly jumps to a much lower value and remains almost constant (though very slowly increasing) for further increases in risk. This effect happens because when the tendency β of the noise source driving the fundamental reaches and surpasses a certain level, the ballistic component in the noise source overcomes the diffusion. The force $\beta \tanh(\beta f)$ in the mean-preserving spread becomes the main driver of the stochastic process driving the fundamental, and therefore f_t becomes a ballistic-driven process with a tendency to escape from its mean that is stronger than the tendency to diffuse around

Figure 5 Risk, target band and regime shifts

Regime shift and eigenvalue jump as a function of risk, for different target bands



its central value. While this may look like a sudden emergence of supercredibility, this is in fact the opposite: the target zone *de facto* ceases to exist, since the bounds cannot be felt even in an infinitesimal time interval dt . The ballistic tendency of the fundamental to escape its initial position causes the band to be hit and even surpassed at every time step, and smooth-pasting conditions cannot be applied anymore. This has a direct implication for honeymoon effects: Appendix B shows how after a threshold level of risk the smooth fitting procedure at the boundaries cannot be applied, and hence honeymoon effects become unobtainable. Since the exchange rate has become primarily ballistic-driven (we remind that ballistic means with variance increasing quadratically in time), this implies that very large risk denies central banks the monetary autonomy until the moment of entering the currency zone. This phenomenon is illustrated in Figure 6.

Consider now the smooth-pasting conditions (10): one can separate the contribution of the eigenfunction to the one given by the probability spread and obtain

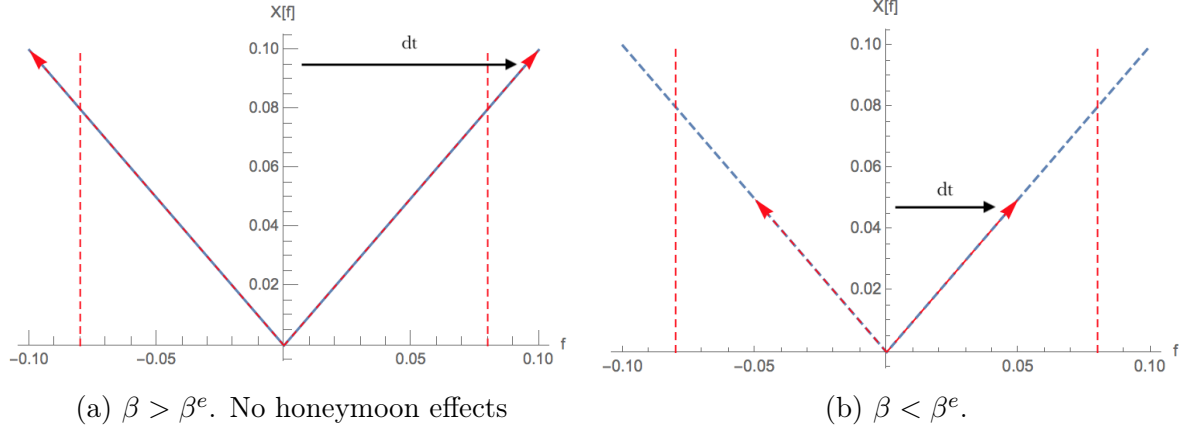
$$\begin{aligned}
 \frac{\partial_f \sin\left(\frac{\sqrt{2}\Omega_k}{\sigma} f_t\right)}{\sin\left(\frac{\sqrt{2}\Omega_k}{\sigma} f_t\right)} - \beta \tanh(\beta f_t) &= 0 \\
 \Updownarrow \\
 \frac{\partial_f \text{EIG}(\Omega_k, f_t)}{\text{EIG}(\Omega_k, f_t)} - \text{MPS}(\beta, f_t) &= 0.
 \end{aligned} \tag{14}$$

The first term is a total sensitivity term, closely related to the elasticity of the eigenfunction with respect to the fundamental, and it represents the overall variation of the exchange rate with the fundamental. The second term represents the increase in risk, as well as the ballistic component that represents the tendency of the fundamental to hit the target bands. The solution of this equation yields the spectrum $\{\Omega_k\}$, for $k = \mathbb{N}^+$. The difference of the two terms represents the residual tendency of the home country fundamental to avoid converging to the target fundamental. The spectral gap, therefore, represents the intensity of the probability spread. The regime shift will happen at a threshold value β^e , only obtainable numerically, for which the spectral gap will suddenly jump upwards: the ballistic repulsive force has dominated over the diffusive part and the first eigenvalue jumps higher. The oscillating part of the expansion increases in frequency, and the time-dependent exponential decay increases in speed. A graphical illustration is shown in Figure 7: one can easily show that the lower bound for the threshold β^e is given by

$1/\bar{f}$. This allows to uncover the close relationship between the regime shift and the size of the target band. This regime shift can not occur with any Gaussian process, as well as with any mean-reverting dynamics.

Figure 6 Risk threshold, distance to the bands and honeymoon effects

Ballistic-driven vs. diffusion-driven regimes



In the diffusion-driven regime (characterised by a relatively low $\beta < 1/\bar{f}$), one observes that an increase of the risk implies a decrease in the sensitivity, since t_{relax} is increasing. This may seem counterintuitive: but it must be remembered that at time $t = 0$, the initial condition is the stationary solution of the central bank-controlled diffusion for the given risk. Increasing β , therefore, is likely to load the stationary probability mass accumulated in the vicinity of on the zone boundaries. Escape from this stationary state by bank action becomes somehow more difficult, ultimately leading to an increase of t_{relax} . Conversely, in high risks regimes $\beta > 1/\bar{f}$ where the ballistic dynamics dominate, the boundaries of the target zone are systematically hit by the fundamental. In this situation, the central bank will intervene almost entirely intramarginally regardless of whether the fundamental is actually close to the bands, since honeymoon effects cannot exist anymore. This allows in Eq.(12) for a sudden reduction of the the probability mass located on the bounds, and this generates the sharp drop of t_{relax} . In other words, the band implicitly ceases to exist and the central bank operates effectively in an infinitesimally narrow band. This opens a different angle on understanding target zone credibility: if risk is too high, exchange rate expectations are no longer anchored to the band and the effectiveness of central bank intervention is greatly damped. What the central bank could do is therefore either reduce risk, which in practice is often infeasible, or increase the size of the target zone which itself is bounded by the free-float exchange rate volatility. The new size of the band would have to be large enough for this new target zone to be “heard”.

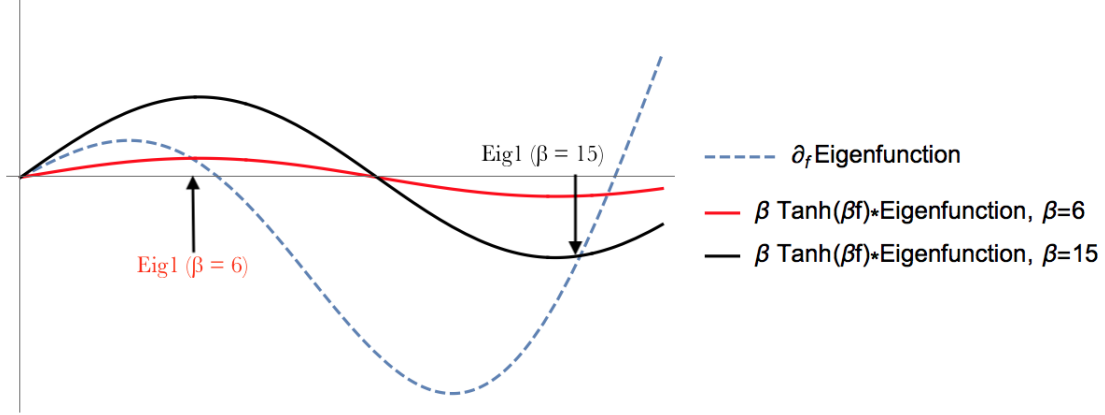
6 Numerical simulations

We simulate central bank intervention by means of a symmetrized Euler scheme for stochastic differential equations. Since the original problem is an one-dimensional Neumann problem on the boundary $\partial D = [-\bar{f}, \bar{f}]$, the regulated SDE can be written as

$$f_t = \int_0^t b(f_s)ds + \sigma \int_0^t dW_s + \int_0^t \gamma(f_s)ds,$$

Figure 7 Risk and eigenvalue jump

Note: Regime change For $\beta = 15$, the repulsive force $\beta \tanh(\beta f)$ (black curve) overcomes the diffusion component and generates the first eigenvalue jump. For $\beta = 6$ (red curve), the regime has not yet shifted. Here $\bar{f} = 0.1$, $\sigma = 1$, $\alpha = 200$, $r = 0.5$.



where $b(f_s)$ is the nonlinear drift and $\gamma(\cdot)$ is the oblique reflection of the process on the boundary ∂D . This is the equivalent of the interventions, and we assume that for the unit vector field γ there exists a constant c so that $\gamma(x) \cdot \vec{n}(x) \geq c$ for all points x on the boundary D . This can be interpreted as assuming bounded interventions. We use a regular mesh $[0, T]$ for the numerical simulation, for which the weak error is of order 0.5 when the reflection is normal (i.e. $\gamma = \vec{n}$), which is our case. We choose this method in order to obtain consistent Monte Carlo simulation of the resulting densities. The algorithm starts with $f_0 = 0$ and for any time t_i for which $f_{t_i} \in D$ we have for $t \in \Delta t = t_{i+1} - t_i$ that

$$F_t^{N,i} = f_{t_i}^N + \hat{b}(f_{t_i}^N)(t - t_i) + \sigma(W_t - W_{t_i})$$

as in the standard Euler-Maruyama scheme, and the nonlinear drift $b(\cdot)$ is approximated with a second-order stochastic Runge-Kutta method. If $F_{t+1}^{N,i} \notin \partial D$, then we set

$$f_{t+1}^N = \pi_{\partial D}^\gamma(F_{t+1}^{N,i}) - \gamma(F_{t+1}^{N,i}),$$

where $\pi_{\partial D}(x)$ is the projection of x on the boundary ∂D parallel to the intervention γ . If $F_{t+1}^{N,i} \in \partial D$, then obviously $f_{t+1}^N = F_{t+1}^{N,i}$. For more references we refer to [Bossy et al. \(2004\)](#). The exchange rate path is then obtained simply by setting $X_t^N = X^*(f_t^N, T - t)$ for every $t \in [0, T]$. It's of fundamental importance to set Δt equal to the update ratio given by $1/\alpha$ in our model, so the increment of the simulated exchange rate path has the same updating time frequency as the central bank. We can now discuss two kinds of intervention: the kind that intervenes by reflecting the process just so it stays within the band (sometimes called “leaning against the wind”), and the pure reflection one, which projects the fundamental process by an amount equivalent to how much the process would have surpassed the boundary. This distinction can be understood also as the amount of how much reserves the central bank has at its disposal in order to stabilize the fundamental process: the greater this amount, the more likely it is that the intervention will be a pure reflection one. We also assume that intervention is effective instantaneously. This distinction has also important implications in the resulting exchange rate density: as shown in [Figure 6](#), given our rigorous characterization of risk, the greater the β and the earlier will the central bank have to intervene, given the fundamental's increased tendency to escape towards the bands. We present five possible scenarios by estimating Monte Carlo densities of the simulated exchange rate process: the first two correspond to the Gaussian case,

where $\beta = 0$ with each of the two intervention strategies. The densities are obtained by Monte Carlo simulation of N sample paths, binning the data and limiting the bin size to zero to obtain the convolution density, then averaging over the N realizations and interpolating the resulting points. For all figures N is set to 5000, $\sigma = 0.1$, $r = 0.5$, $\alpha = 200$, $T = 3$, exchange rate target band $\pm 10\%$. For more references on the method we refer to [Asmussen and Glynn \(2007\)](#). We obtain a realization path for each of the two and obtain both U-shaped (corresponding to the base Krugman case) and hump-shaped densities, corresponding to the [Dumas and Delgado \(1992\)](#) framework. The realized densities are shown in Figure 8. We then simulate the case in which $\beta > 0$ but not large enough to trigger the regime shift, each one with a different intervention strategy: in the marginal intervention case we obtain the two-regime density ($\beta = 5$), as in the [Bessec \(2003\)](#) framework, and in the intramarginal one we obtain a hump-shaped distribution as for all intramarginal intervention frameworks. These results are shown in Figure 9. We now note that this is a consequence of our characterization of risk: the tendency β of the fundamental to hit the boundary generates the two-regime shape, since even in a marginal framework the central bank will intervene already when at a distance to the bands. Furthermore, this is the case in which *de facto* bands start to appear. Finally, we present a case in which β is large enough ($\beta = 50$) to trigger the regime shift, and the band in fact ceases to exist: the tendency to escape brings the fundamental process to constantly surpass the boundary, honeymoon effects are impossible and pure reflection intervention concentrates most of the realizations around the initial level. This, as $N \rightarrow \infty$, generates a Dirac delta function around the initial value of the fundamental. This is shown in Figure 10.

Figure 8 Exchange rate densities, $\beta = 0$

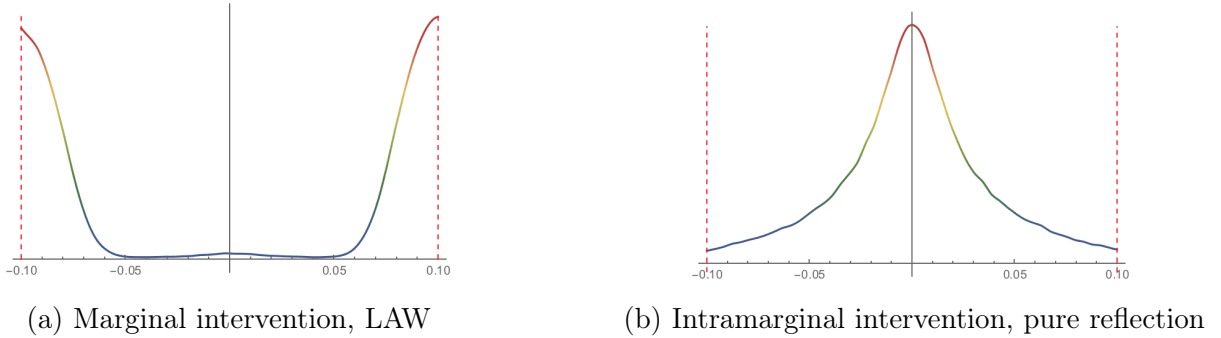
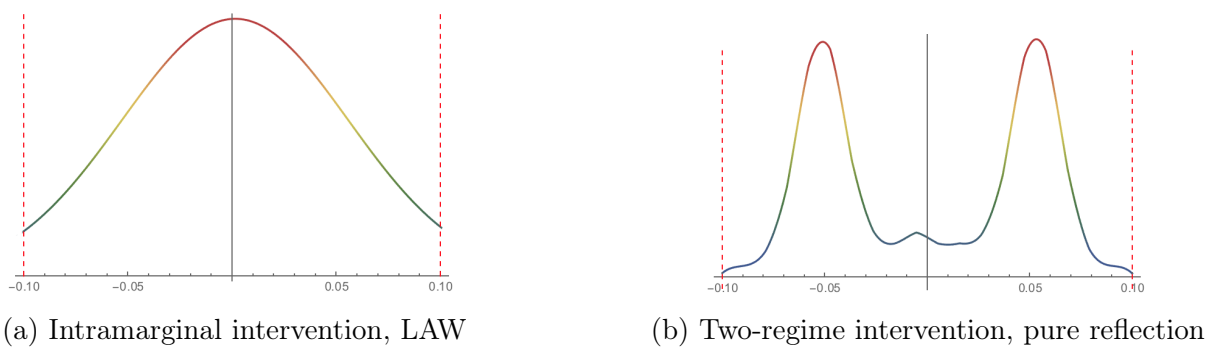


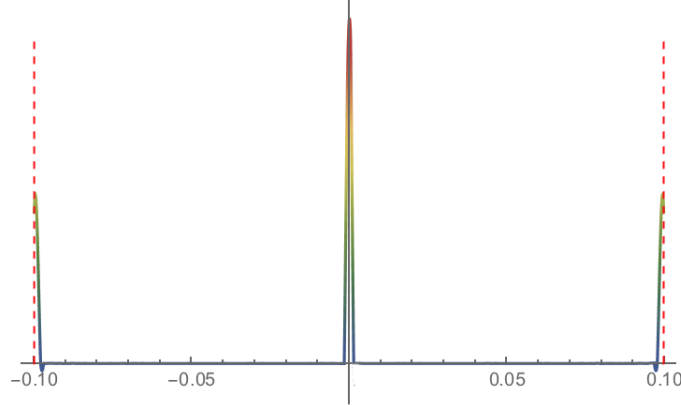
Figure 9 Exchange rate densities, $\beta > 0, \beta < \beta^e$



7 Sources of risk

Let us now explore the implications of our characterization of fundamental risk. Up to now we have chosen to keep β as purely a parameter of increasing risk, which controls the probability

Figure 10 Exchange rate densities, $\beta > \beta^e$,



Ballistic regime dominates and target band too narrow given the level of risk.

spread and hence the tails of the fundamental distribution. What we want to achieve in this section is to connect this parameter to specific economic mechanisms which may drive the determination of exchange rate dynamics. [Rey \(2015\)](#) and [Kalemli-Ozcan *et al.* \(2019\)](#) study the role of the global financial cycle in exchange rate arrangements. According to these developments, the trilemma configuration of monetary policy, exchange rate regime and capital mobility is determined by country-specific risk and is affected by global risk aversion. One of the key assumptions of the literature is the fulfillment of the no-arbitrage condition, usually modeled by UIP. However, a vast empirical literature shows that UIP does not hold. Such deviations from the UIP conditions are shown to be correlated with risk:

$$\mathbb{E} \left(\frac{dX_t}{dt} \right) = g(i_t^* - i_t) + \eta,$$

where g is a weakly increasing function, generally taking small values, i^* is the anchor country interest rate and η is the UIP deviation. From the financial crisis literature - see for example [Miranda-Agrippino and Rey \(2019\)](#) and [Avdjiev *et al.* \(2019\)](#) - this deviation is shown to be directly determined by

$$\eta = i^* + \gamma,$$

where γ is country-specific risk. The literature largely ignores this fact, given the modeling choices in the fundamental process which tend to model risk only indirectly, either via realignment risk or by adding jumps to the process. One potential interpretation of the parameter of increasing risk β is to account for the extra risk stemming from the failure of the arbitrage condition and for country-specific risk. It is clear that as country risk increases, it is more difficult for the country fundamental to converge to the target fundamental.

Another possible interpretation of β is by exploring the other source of UIP deviations: capital flows. It is well-known that capital flows are procyclical with global risk aversion, and therefore affecting the magnitude of the deviation. To give a stylized description, consider the fundamental process of the exchange rate as defined by

$$f_t = m_t + v_t$$

where m_t is the money supply and a general stochastic process $v(t)$ which is a composite money demand shock (“velocity”). Usually money supply is assumed constant: in our case, however, we include the potential of domestic money supply being affected by exogenous foreign money supply

shocks, as proxied by incoming capital flows. Note that this source of risk cannot be modeled by adding more Gaussian noise, or by modulating the variance (see Appendix C for an illustration of this fact). We assume here that the central bank is using unsterilized intervention to lean against the direction of capital flows. This also implies that the only channel of adjustment is the interest rate differential: this is in line with [Lai et al. \(2008\)](#), who show that the relationship between the interest rate differential and exchange rate dynamics can have a correlation structure that is not necessarily negative. For open economies, the magnitude by which domestic money supply is affected by foreign fundamentals is determined by the measure of capital mobility allowed by the home country. Let us therefore define the deviation from UIP parity as

$$\Delta UIP_t(\beta) = \beta \left(i_t - i_t^* - \mathbb{E} \frac{X_t}{dt} \right), \quad (15)$$

where β is a measure of capital mobility, i the domestic interest rate and i^* is the reference rate. Note that when $\beta = 0$ this deviation is zero by construction, and when β is very high UIP needs to hold because of the high degree of capital flows which implies a fast convergence of the interest rate differential. Note also that in both of these cases we revert to the Krugman case if one allows constant infinitesimal marginal intervention. If (15) is nonzero, using the fundamental exchange rate equation one immediately obtains that the exchange rate X is determined by its fundamental equation plus an amount proportional to the deviation, i.e.

$$X_t = r f_t + \frac{(1-r)}{\alpha} \mathbb{E} \left\{ \frac{dX_t}{dt} \right\} + g(\Delta UIP_t(\beta))$$

where $g(\cdot)$ is a general nondecreasing function (scaled by r). In a target zone setting, if the domestic money supply m_t is not constant and subject to exogenous shocks given by capital flows, then monetary authorities have to react in such a way as to counteract exchange market pressures created by the capital flows themselves in order to maintain the zone. The mean of this deviation in a target zone, therefore, should be zero. Since the variation of this deviation is always non-zero, we are therefore augmenting the fundamental process by means of a *mean-preserving spread*, calibrated by the degree of capital mobility β .

We can therefore also connect the threshold β_e at which the regime shift occurs to complete factor market integration: for lower levels of β , the home fundamental exhibits an idiosyncratic component anchored to its original dynamics that is stronger than its tendency to converge to the target fundamental. Once this component is overcome, the target zone ceases to exist and the currency starts floating. This also may help explaining why countries with a high level of capital integration with the target currency may have higher costs in maintaining a target zone. One implication of the suddenness of the regime shift is that the relationship between capital integration and the duration of the target zone is non-monotonic. This is precisely what [Lera and Sornette \(2015\)](#) illustrate with the case of the Swiss Franc floor between 2011-2015.

7.1 Policy implications and potential contributions

A target zone with a terminal exit time to another currency has two objectives. First, the central bank wants to limit the volatility of the its exchange rate (X_t) versus the anchor currency below the free float level of the anchor currency (Z_t). This provides us a natural limiting condition to the size of the band that the central bank can set.

$$|\bar{f}| \leq \sigma_z$$

This essentially means that the band size of ERM-II of $\pm 15\%$ will never be breached if the central bank of the target zone currency pegs to the Euro, as the Euro itself has a annualised volatility versus other major currencies in the range of 7-10%. Second, the central bank needs its target-zone to be considered credible, to enjoy “honeymoon effects”, which in turns reduces the cost of intervention for achieving the set parity. In our setup, we uncover the concept of a characteristic relaxation time τ_{relax} which determines the minimum time a target zone must be maintained to “feel” the first effects of the home central bank’s actions aimed at reducing fluctuations of the exchange rate, compared to a free float.⁹ This allows us to interpret τ_{relax} as the minimum time for agents for update their previously held exchange rate expectations, generating self-fulfilling expectations that create the honeymoon effect.

This does not mean that a central bank can’t adopt a target currency overnight with an arbitrary parity being the close of day value of the target exchange rate. In such a case, agents would not have had time to update their expectations and this would force the central bank to use a larger proportion of its assets (in the target currency) defending the parity level. This opens up many different avenues of enquiry into the expectation generation process of agents in foreign exchange markets. If t_{relax} as the minimum time for agents for update their previously held exchange rate expectations, this means that a higher degree of agent risk aversion will reduce t_{relax} . As shown by Osler (1995), this effect would work through the credibility of the target zone in time shifting speculators’ horizons towards short term speculation, where $t_{speculation} \leq t_{relax}$. This is a natural outcome of “honeymoon effects” which make intervention cheaper for central banks and harder for speculators after t_{relax} .

We find that t_{relax} is increasing in riskiness of the fundamental process for $\beta \leq \beta_e$. Moreover, the target band size is also increasing in riskiness of the fundamental process for $\beta \leq \beta_e$ up to $|\bar{f}| \leq \sigma_z$.

A potential relevance of our framework may have emerged in a recent development for the Economic Community of West African States (ECOWAS). ECOWAS is planning to replace the current West African CFA Franc with a common currency, named Eco. The goal is for the 15 states to transition to the Eco via a target zone mechanism, similar to the ERM-II. Currently the CFA Franc is pegged to the Euro, with operational management shared between the Bank of France and the local central banks. After the reform, these countries would have to manage their own exchange rate targets without any outside support. The main economic and reasons are understandable, and lie primarily in boosting cross-border trade and economic development in the African sub-region, and in the severing of the ties with the former colonial ruler, France. One of the main concerns is the short time horizon proposed for the target zone mechanism (one year). Moreover, there may be additional risk stemming from not allowing the ECB to have operational risk-sharing in the process, as well as the inherent risk faced by individual West African central banks. This translates directly to our framework, where the risk factor β may generate a relaxation time t_{relax} for individual states that may be larger than the proposed convergence time T . This could potentially have devastating consequences on the credibility of the participating central banks, and of the overall process of creation of the new common currency. The inability of some ECOWAS countries to achieve the convergence criteria would make the adoption of ECO impossible in the near future.

⁹The bank’s actions may be then viewed as a *de facto* reduction of the target zone band over time, whilst the *de jure* band remains unchanged.

8 Conclusions

In this paper we have explored the implications of extending exchange rate target zone modeling to non-stationary dynamics and a more rigorous definition of risk. Our framework leads to a natural interpretation of target zone credibility, driven by the interplay between two contrasting forces: a destabilizing ballistic effect driven by risk which pushes the exchange rate towards the bands, and a stabilizing diffusive force.

Our model does not deal with optimal choices: indeed, the only choice variable potentially available to the authorities is the time horizon T by when the required parity needs to obtain. As such, from the policy perspective our model poses what is essentially a screening problem in the informational sense: in a worst case scenario, it is likely that neither of the two central banks knows the true riskiness of the fundamental process. If one chooses an exit time which is lower than the required minimum time at which parity can be reached (the relaxation time), the target zone exit time is not credible. However, setting a T which is too high exposes one to increased business cycle risks, the dampening of which were a likely reason for entering a target zone in the first place. We show how our model effectively endogenizes the presence of the bands by the exchange rate expectations, and how the interplay between risk and target band has key implications in the credibility of the zone itself, as well as the possibility of honeymoon effects. Intervention is shown to be both marginal and intramarginal, depending on how much the central bank “hears” the distance to the target zone band. The potential emergence of regime shifts, furthermore, can further erode the target zone credibility, and would prompt the central bank to either intervene. This allows the methods employed in this paper to be applied to a wide range of situations. An important future contribution of our work would be the structural estimation of the model parameters and an explicit computation of the relaxation time, thus effectively providing a lower bound for the necessary time for a country to reach the desired parity.

References

- Ajevskis V (2011). “A target zone model with the terminal condition of joining a currency area.” *Applied Economics Letters*, **18**(13), 1273–1278.
- Ajevskis V (2015). “An Exchange Rate Target Zone Model with a Terminal Condition and Mean-Reverting Fundamentals.” *Papers*, arXiv.org. URL <https://EconPapers.repec.org/RePEc:arx:papers:1506.04880>.
- Arcand JL, Hongler MO, Rinaldo D (2019). “Increasing risk: Dynamic mean-preserving spreads.” *Journal of Mathematical Economics*.
- Asmussen S, Glynn PW (2007). *Stochastic simulation: algorithms and analysis*, volume 57. Springer Science & Business Media.
- Avdjiev S, Bruno V, Koch C, Shin HS (2019). “The dollar exchange rate as a global risk factor: evidence from investment.” *IMF Economic Review*, **67**(1), 151–173.
- Bekaert G, Gray SF (1998). “Target zones and exchange rates:: An empirical investigation.” *Journal of International Economics*, **45**(1), 1–35.
- Bertola G, Caballero R (1992). “Target Zones and Realignment.” *American Economic Review*, **82**(3), 520–36. URL <https://EconPapers.repec.org/RePEc:aea:aecrev:v:82:y:1992:i:3:p:520-36>.
- Bertola G, Svensson LEO (1993). “Stochastic Devaluation Risk and the Empirical Fit of Target-Zone Models.” *The Review of Economic Studies*, **60**(3), 689–712. ISSN 0034-6527. <http://oup.prod.sis.lan/restud/article-pdf/60/3/689/4468860/60-3-689.pdf>, URL <https://doi.org/10.2307/2298131>.
- Bessec M (2003). “Mean-reversion vs. adjustment to PPP: the two regimes of exchange rate dynamics under the EMS, 1979–1998.” *Economic Modelling*, **20**(1), 141–164.
- Bossy M, Gobet E, Talay D (2004). “A symmetrized Euler scheme for an efficient approximation of reflected diffusions.” *Journal of applied probability*, **41**(3), 877–889.
- Chinn MD, Moore MJ (2011). “Order flow and the monetary model of exchange rates: Evidence from a novel data set.” *Journal of Money, Credit and Banking*, **43**(8), 1599–1624.
- Coibion O, Gorodnichenko Y (2015). “Information rigidity and the expectations formation process: A simple framework and new facts.” *American Economic Review*, **105**(8), 2644–78.
- Crespo-Cuaresma J, Égert B, MacDonald R (2005). “Non-Linear Exchange Rate Dynamics in Target Zones: A Bumpy Road Towards A Honeymoon Some Evidence from the ERM, ERM2 and Selected New EU Member States.” *William Davidson Institute Working Papers Series wp771*, William Davidson Institute at the University of Michigan. URL <https://ideas.repec.org/p/wdi/papers/2005-771.html>.
- Dumas B, Delgado F (1992). “Target zones, broad and narrow.” *Exchange rate targets and currency bands*.
- Evans MD (2010). “Order flows and the exchange rate disconnect puzzle.” *Journal of International Economics*, **80**(1), 58–71.
- Evans MD, Lyons RK (2002). “Order flow and exchange rate dynamics.” *Journal of political economy*, **110**(1), 170–180.
- Ferreira A, Moore M, Mukherjee S (2019). “Expectation Errors in the Foreign Exchange Market.” *Journal of International Money and Finance*, **95**, 44–51.
- Gopinath G, Stein J (2019). “Banking, Trade and the Making of a Dominant Currency.” Under revision for the Quarterly Journal of Economics.
- Kac M (1966). “Can one hear the shape of a drum?” *The american mathematical monthly*, **73**(4P2), 1–23.

- Kalemli-Ozcan S, Varela L, *et al.* (2019). “Exchange Rate and Interest Rate Disconnect: The Role of Capital Flows, Currency Risk and Default Risk.” In “2019 Meeting Papers,” 351. Society for Economic Dynamics.
- Kalemli-Özcan e (2019). “U.S. Monetary Policy and International Risk Spillovers.” *Working Paper 26297*, National Bureau of Economic Research. URL <http://www.nber.org/papers/w26297>.
- Krugman PR (1991). “Target zones and exchange rate dynamics.” *The Quarterly Journal of Economics*, **106**(3), 669–682.
- Lai Cc, Fang Cr, Chang Jj (2008). “Volatility trade-offs in exchange rate target zones.” *International Review of Economics & Finance*, **17**(3), 366–379.
- Lera SC, Leiss M, Sornette D (2019). “Currency target zones as mirrored options.”
- Lera SC, Sornette D (2015). “Currency target-zone modeling: An interplay between physics and economics.” *Physical Review E*, **92**(6), 062828.
- Lera SC, Sornette D (2016). “Quantitative modelling of the EUR/CHF exchange rate during the target zone regime of September 2011 to January 2015.” *Journal of International Money and Finance*, **63**, 28–47.
- Lera SC, Sornette D (2018). “An explicit mapping of currency target zone models to option prices.” *International Review of Finance*.
- Linetsky V (2005). “On the transition densities for reflected diffusions.” *Advances in Applied Probability*, **37**(2), 435–460.
- Lundbergh S, Teräsvirta T (2006). “A time series model for an exchange rate in a target zone with applications.” *Journal of Econometrics*, **131**(1-2), 579–609.
- Mathieson DJ, Flood R, Rose A (1991). “An Empirical Exploration of Exchange Rate Target-Zones.” *IMF Working Papers 91/15*, International Monetary Fund. URL <https://EconPapers.repec.org/RePEc:imf:imfwpa:91/15>.
- Meese R, Rose A (1991). “An Empirical Assessment of Non-Linearities in Models of Exchange Rate Determination.” *Review of Economic Studies*, **58**(3), 603–619. URL <https://EconPapers.repec.org/RePEc:oup:restud:v:58:y:1991:i:3:p:603-619>.
- Miranda-Agrippino S, Rey H (2019). “US Monetary Policy and the Global Financial Cycle.” *Working Paper 21722*, National Bureau of Economic Research. URL <http://www.nber.org/papers/w21722>.
- Osler CL (1995). “Exchange rate dynamics and speculator horizons.” *Journal of International Money and Finance*, **14**(5), 695–719.
- Rey H (2015). “Dilemma not Trilemma: The Global Financial Cycle and Monetary Policy Independence.” *NBER Working Papers 21162*, National Bureau of Economic Research, Inc. URL <https://ideas.repec.org/p/nbr/nberwo/21162.html>.
- Rothschild M, Stiglitz JE (1970). “Increasing Risk I: A Definition.” *Journal of Economic Theory*, **2**(3), 225–243.
- Rothschild M, Stiglitz JE (1971). “Increasing Risk: II. Its Economic Consequences.” *Journal of Economic Theory*, **3**(1), 66–84.
- Studer-Suter R, Janssen A (2017). “The Swiss franc’s honeymoon.” *University of Zurich, Department of Economics, Working Paper*, (170).
- Svensson LEO (1991). “Target zones and interest rate variability.” *Journal of International Economics*, **31**(1-2), 27–54. URL <https://ideas.repec.org/a/eee/inecon/v31y1991i1-2p27-54.html>.
- Tristani O (1994). “Variable probability of realignment in a target zone.” *The Scandinavian Journal of Economics*, pp. 1–14.
- Werner AM (1995). “Exchange rate target zones, realignments and the interest rate differential: Theory and evidence.” *Journal of International Economics*, **39**(3-4), 353–367.

Appendices

A Derivations of the stationary and transient equations

For the derivation of the stationary solution, we first introduce the following integral transformation:

$$X(t, f) = \int^f \cosh(\beta\zeta) Y(t, \zeta) d\zeta \quad \Longleftrightarrow \quad \partial_f X(t, f) = \cosh(\beta f) Y(t, f), \quad (16)$$

which is Darboux-type functional transformation. Eq.(4) therefore leads to:

$$\partial_t Y(t, f) + \frac{\sigma^2}{2} \partial_{ff} Y(t, f) - \left[\frac{\beta^2}{2} + \frac{\alpha}{(1-r)} \right] Y(t, f) = -\frac{r\alpha}{(1-r)} f \cosh(\beta f). \quad (17)$$

Setting $\partial_t = 0$ one obtains a nonlinear ODE in f which has the closed form solution as given by (7), which is the sum of the general solution (two opposite-sided exponentials) and a particular solution. Inverting the transformation back to X one obtains (6).

For the transient dynamics, we need to solve the following equation:

$$\begin{cases} \partial_\tau X(\tau, f) - \frac{\sigma^2}{2} \partial_{ff} X(\tau, f) - \beta \tanh(\beta f) \partial_f X(\tau, f) + \frac{\alpha}{(1-r)} X(\tau, f) = +\frac{r\alpha}{(1-r)} f, \\ X(0, f) = 0. \end{cases} \quad (18)$$

Writing $X(\tau, f) = X^*(\tau, f) + X_S(f)$, Eq.(18) implies:

$$\begin{cases} -\frac{\sigma^2}{2} \partial_{ff} X_S(f) - \beta \tanh(\beta f) \partial_f X_S(f) + \frac{\alpha}{(1-r)} X_S(f) = +\frac{r\alpha}{(1-r)} f, \\ \partial_\tau X^*(\tau, f) - \frac{\sigma^2}{2} \partial_{ff} X^*(\tau, f) - \beta \tanh(\beta f) \partial_f X^*(\tau, f) + \frac{\alpha}{(1-r)} X^*(\tau, f) = 0. \end{cases} \quad (19)$$

While the first line in Eq.(19) has already being solved in Eq.(6), the second line needs now to be discussed. Writing again $X^*(\tau, f) \cosh(\beta f) := Y^*(\tau, f)$, we obtain:

$$\partial_\tau Y^*(\tau, f) - \frac{\sigma^2}{2} \partial_{ff} Y^*(\tau, f) + \left[\frac{\beta^2}{2} + \frac{\alpha}{(1-r)} \right] Y^*(\tau, f) = 0. \quad (20)$$

The smooth-pasting conditions given by Eq.(8) imposes:

$$\begin{cases} \partial_f X^*(\tau, f) |_{f=\underline{f}} = 0 & \Rightarrow & \{[\partial_f Y^*(\tau, f)] - \beta \tanh(\beta f) Y^*(\tau, f)\} |_{f=\underline{f}} = 0, \\ \partial_f X^*(\tau, f) |_{f=\bar{f}} = 0 & \Rightarrow & \{[\partial_f Y^*(\tau, f)] - \beta \tanh(\beta f) Y^*(\tau, f)\} |_{f=\bar{f}} = 0. \end{cases} \quad (21)$$

We solve (20) by separation of variables and expansion over the basis of a complete set of orthogonal eigenfunctions. The solution can be expressed as $Y^*(\tau, f) = \phi(\tau)\psi(f)$, and therefore we can write it as

$$\frac{\dot{\phi}(\tau)}{\phi(\tau)} = \lambda_k = \frac{\sigma^2}{2} \frac{\psi''(f)}{\psi(f)} - \rho$$

where $\rho = \left[\frac{\beta^2}{2} + \frac{\alpha}{(1-r)} \right]$.

The time-dependent part solves to $\psi(\tau) = \exp(\tau\lambda_k)$, and the fundamental-dependent part can be written as

$$\psi''(f) - 2(\lambda_k + \rho)\psi(f) = \psi''(f) + 2\frac{\Omega_k^2}{\sigma^2}\psi(f) = 0.$$

The rest of the derivations follow straightforwardly, solving for ψ and obtaining the eigenfunctions

$$\psi_k(f) = c_1 \cos\left(\sqrt{2}\frac{\Omega_k}{\sigma}f_t\right) + c_2 \sin\left(\sqrt{2}\frac{\Omega_k}{\sigma}f_t\right).$$

which form an orthogonal basis for the space of $2\bar{f}$ well-behaving functions. Smooth-pasting conditions impose $c_1 = 0, c_2 = 1$ and we obtain the form of the eigenfunctions as given by (11). The Fourier coefficients follow in their standard form, using the stationary equation $X_S(f_t)$.

B Risk, regime shifts and honeymoon effects

We now briefly discuss the connection between risk and honeymoon effect, and how such effects cannot be obtained when the ballistic tendency of the fundamental is too large. For illustrative purposes, let us consider a baseline case of our model with $r = 1/2$ in a symmetric band $[-\bar{f}, \bar{f}]$ around the parity 0, and let us compare the DMPS-driven model with the standard Gaussian one. Omitting time dependency, we have again the framework given by

$$X = f + \frac{1}{\alpha} \frac{\mathbb{E}\{dX\}}{dt},$$

which leads to the following couple of PDEs, depending on the form of the fundamental process.

$$\begin{cases} X = f + \frac{1}{2}\partial_{ff}[X(f)] & \text{(Gaussian),} \\ X = f + \frac{1}{2}\partial_{ff}[X(f)] + \beta \tanh(\beta f)\partial_f[X(f)] & \text{(DMPS).} \end{cases}$$

We now focus on the stationary regime for which get the general solutions:

$$\begin{cases} X(f) = f + A_0 \sinh(\rho_0 f), & \text{(Gaussian),} \\ X(f) = f + A_\beta \frac{\sinh(\rho_\beta f)}{\cosh(\beta f)}, & \text{(DMPS),} \end{cases}$$

where $\rho_\beta = \sqrt{\beta^2 + 4\alpha}$ and A_β is a yet undetermined amplitude. We now apply the smooth fitting procedure at the target level $+\bar{f}$ ¹⁰. Accordingly we have:

$$\begin{cases} X(F) := \hat{X} = F + A_0 \sinh(\rho_0 F), & \text{(fitting at level } F), \\ 0 = 1 + A_0 \rho_0 \cosh(\rho_0 F) & \text{(smooth fitting),} \end{cases}$$

Accordingly we have:

$$\hat{X} = \bar{f} - \frac{\sinh(\rho_0 \bar{f})}{\rho_0 \cosh(\rho_0 \bar{f})} \rightarrow \hat{X} > \bar{f}.$$

The fact that $\hat{X} > \bar{f}$ is a direct consequence of the honeymoon effect.

We now show how our characterization of risk changes radically the above framework. We perform the smooth fitting for the DMPS process and obtain:

$$\begin{cases} X(\bar{f}) := \hat{X} = \bar{f} + A_\beta \frac{\sinh(\rho_\beta \bar{f})}{\cosh(\beta \bar{f})}, & \text{(fitting at level } \bar{f}), \\ 0 = 1 + \frac{A_\beta}{\cosh^2(\beta \bar{f})} [\rho_\beta \cosh(\rho_\beta \bar{f}) \cosh(\beta \bar{f}) - \beta \sinh(\beta \bar{f})] & \text{(smooth fitting).} \end{cases}$$

¹⁰Due to the symmetry, we have here only one amplitude A to determine since only one boundary needs to be considered.

Accordingly, we now obtain:

$$\hat{X} = \bar{f} - \cosh(\beta \bar{f}) \frac{\sinh(\rho_0 \bar{f})}{\underbrace{\rho_\beta \cosh(\beta \bar{f}) \cosh(\rho_0 \bar{f}) - \beta \sinh(\beta \bar{f}) \sinh(\rho_\beta F)}_{\mathcal{A}(\beta)}}.$$

Now we have to distinguish between two regimes. i) $\mathcal{A}(\beta) < 0$ and conversely ii) $\mathcal{A}(\beta) > 0$. The transition between these two regimes occurs when $\mathcal{A}(\beta) = 0$, that is to say:

$$\rho_\beta \cotanh(\rho_\beta \bar{f}) = \beta \tanh(\beta \bar{f}). \quad (22)$$

Now we observe that the singularity observed in Eq.(22) coincides with Eq.(11) which in our manuscript precisely determines the lowest eigenvalue of the spectrum. In other words, for β large enough, the smooth-fitting procedure cannot be applied, and hence it exists a critical risk level β^e for which the honeymoon effect cannot possibly apply.

C Noise sources driving the fundamental

Let us now assume that the fundamental is driven by a couple of noise sources, namely i) composite shocks v_t and ii) fluctuations in the money supply m_t , given by Gaussian noise around a drift μ . We therefore add another source of noise, but we are not necessarily increasing the risk in the fundamental process. We then have

$$\begin{cases} df_t = \sigma_1 dW_{1,t} + dm_t, \\ dm_t = \mu dt + \sigma_2 dW_{2,t}, \quad m_{t=0} = m_0. \end{cases} \quad (23)$$

where the noise sources $dW_{1,t}$ and $dW_{2,t}$ are two independent White Gaussian Noise (WGN) processes. We then obtain f_t as a Gaussian process, since trivially

$$df_t = \mu dt + \sqrt{\sigma_1^2 + \sigma_2^2} dW_t$$

and we are exactly in the standard framework (in the literature usually $\mu = 0$), only with a change in variance. If however we wish to incorporate a general increase in risk, and one that may represent the repulsive force that was discussed in Section 2, we can write the following more general framework:

$$\begin{cases} df_t = \sigma_1 dW_{1,t} + dm_t, \\ dz_{\beta,t} = \zeta(\beta; z_t) dt + \sigma_2(\beta) dW_{2,t}, \quad z_{t=0} = 0. \end{cases}$$

where $\beta \geq 0$ is a control parameter and the repulsive drift $\zeta(\beta; z) = -\zeta(\beta; -z) < 0$ models an extra risk source via a dynamic zero mean process. We parametrize risk with β , and therefore $\beta = 0$ simply implies $\sigma_2(\beta) = \zeta(0; z_t) = 0$ implying that the process is Gaussian and driven entirely by the composite shock process. Our candidate for ζ is the DMPS process:

$$df_t = \sigma_1 dW_{1,t} + dz_t = \beta \tanh(\beta z_t) dt + \sigma_1 dW_{1,t} + \sigma_2(\beta) dW_{2,t}$$

\Downarrow

$$dz_t = \beta \tanh(\beta z_t) dt + \left[\sqrt{\sigma_1^2 + \sigma_2^2(\beta)} \right] dW_t, \quad z_{t=0} = 0.$$

where we used the fact that the difference between two independent WGN's is again a WGN with variance as given in the previous equation. Alternatively one may formally write:

$$df_t = \sigma_1 dW_{1,t} + \beta \tanh \left[\overbrace{\beta (f_t - \sigma_1 W_{1,t})}^{z_t} \right] dt + \sigma_2(\beta) dW_{2,t} =$$

$$\beta \tanh \left[\overbrace{\beta (f_t - \sigma_1 W_{1,t})}^{z_t} \right] dt + \left[\sqrt{\sigma_1^2 + \sigma_2^2(\beta)} \right] dW_t,$$

Using the initial equation (1) and the previous equation and applying Itô's lemma to the functional $X(f_t, t)$, we obtain:

$$\frac{(1-r)}{\alpha} \left\{ \partial_t X(f, t) + \partial_f X(f, t) \underbrace{\mathbb{E} \{ \beta \tanh [\beta (f_t - \sigma_1 W_{1,t})] \}}_{=\beta \tanh[\beta(f)]} + [\sigma_1^2 + \sigma_2^2(\beta)] \partial_{ff} X(f, t) \right\} =$$

$$X_t - r f_t$$
(24)

In the last Eq.(24), the under-brace equality follows since all odd moments in the expansion of the hyperbolic tangent vanish and the $\tanh(x)$ is itself an odd function. Now, normalizing as to have $[\sigma_1^2 + \sigma_2^2(\beta)] = 1$, we are in the nominal setting of our paper.

D Attracting drift: mean-reverting dynamics

A fully similar discussion can be done for mean-reverting fundamental dynamics (Ornstein-Uhlenbeck dynamics) reflected inside an interval $[\underline{f}, \bar{f}]$. In this section, the fundamental is driven by the mean-reverting dynamics:

$$df = \theta(\mu - f)dt + \sigma dW_t,$$

where μ is the “long-run” level of the fundamental, and θ is the speed of convergence. Following the previous exposition, we can obtain the full solution for the exchange rate $X^*(t, f)$ as the solution of

$$\partial_t X + \frac{\sigma^2}{2} \partial_{ff} X + \theta(\mu - f) \partial_f X - \frac{\alpha}{1-r} X = -\frac{r\alpha}{1-r} f.$$

As before, we have the stationary solution for a vanishing ∂_t , and here it reads

$$X_S(f) = A {}_1F_1 \left[\frac{\alpha}{2\theta(1-r)}, \frac{1}{2}; \frac{\theta}{\sigma^2} (f - \mu)^2 \right] +$$

$$+ B \frac{\sqrt{\theta}}{\sigma} (f - \mu) {}_1F_1 \left[\frac{\alpha}{2\theta(1-r)} + \frac{1}{2}, \frac{3}{2}; \frac{\theta}{\sigma^2} (f - \mu)^2 \right] +$$

$$+ \left[\frac{\theta\mu(1-r)f + r\alpha}{\theta(1-r) + \alpha} \right]$$
(25)

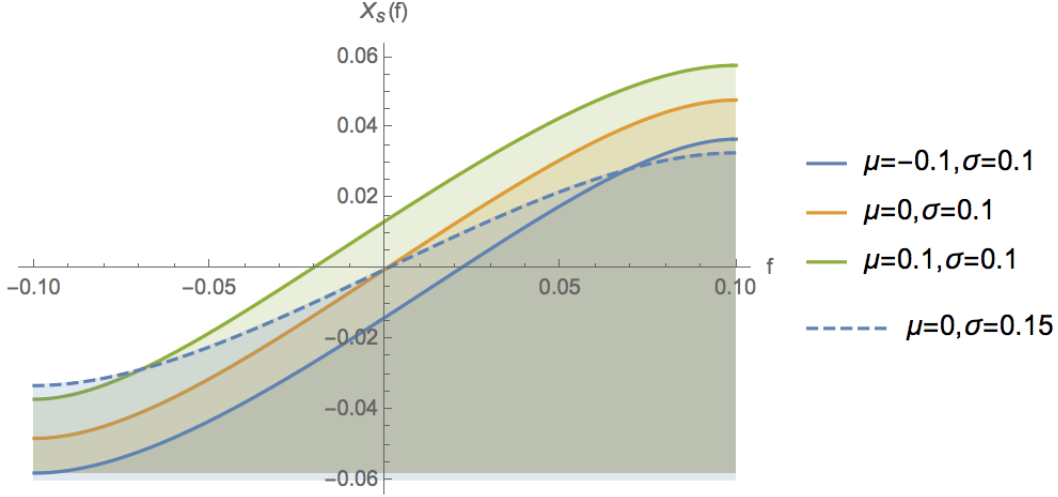
where ${}_1F_1[a, b; x]$ is the confluent hypergeometric function. The integration constants A and B , as before, are determined via smooth pasting at the target zone boundaries, namely: $\partial X_S(f)|_{f=\underline{f}} = \partial X_S(f)|_{f=\bar{f}} = 0$. Note that if $\mu = 0$, then $A = 0$. Figure 11 shows the stationary dynamics of the exchange rate as function of the fundamental, for different values of long-run level μ and noise variance σ . The band is assumed symmetric around 0, and $\bar{f} = 10\%$.

The associated Sturm-Liouville equation is now given by

$$\frac{\sigma^2}{2} \partial_{ff} X + \theta(\mu - f) \partial_f X + \rho X = 0,$$

where $\rho = \frac{\alpha}{1-r}$, and the spectrum of the process can be obtained explicitly by solving a transcendental equation involving Weber parabolic cylinder functions. As before, the complete solution is given by an expansion on a complete set of orthogonal functions on the target band, namely:

Figure 11 Mean-Reverting Stationary Dynamics



$$X^*(T-t, f) = X_S(f) + \sum_{k=1}^{\infty} c_k \exp[-(\Omega_k + \rho)(T-t)] \psi(\Omega_k, f),$$

where the Fourier coefficients c_k again impose the terminal condition $X^*(0, f) = -X_S(f)$. As worked out by Linetsky (2005) explicit though lengthy closed form expressions are obtainable (see Eqs.(39) and (40)). For the case of a symmetric target zone $\underline{f} = -\bar{f}$, an approximation valid for large eigenvalues Ω_k , (i.e. large k 's) is given in [L] and reads:

$$\begin{aligned} \Omega_k &= \frac{k^2 \pi \sigma^2}{8 \bar{f}^2} + \frac{\theta}{2} + c_0 + O\left(\frac{1}{k^2}\right) \\ c_0 &= \frac{\theta^2}{6 \sigma^2} (4 \bar{f}^2 - 6 \bar{f} \mu + 3 \mu^2). \end{aligned} \quad (26)$$

The normalised eigenfunctions, also up to $O\left(\frac{1}{k^2}\right)$, read:

$$\begin{aligned} \psi_k(f) &= \pm \frac{\sigma}{\sqrt{2}} \bar{f}^{-1/2} \exp\left[\frac{\theta(f-\mu)^2}{2\sigma^2}\right] \left[\cos\left(\frac{k\pi f}{2\bar{f}}\right) + \frac{2\bar{f}}{k\pi\sigma^2} \phi(f) \sin\left(\frac{k\pi f}{2\bar{f}}\right) \right] \\ \phi(f) &= \frac{\theta^2}{6\sigma^2} f^3 - \frac{\theta^2 \mu}{2\sigma^2} f^2 - \left[\frac{\theta}{2} \left(\frac{\sqrt{2\theta}}{\sigma} \mu + 1 + c_0 \right) \right] f + \theta \mu \end{aligned} \quad (27)$$

While strictly speaking Eq.(26) furnishes very good estimates for large k values, a closer look in [L] shows that even for low k 's, ($k = 1, 2, \dots$), pretty good approximations are also obtainable. In particular, for $k = 1$, we approximately have:

$$\tau_{\text{relax}} \simeq [\Omega_1]^{-1} = \left[\frac{\pi \sigma^2}{8 \bar{f}^2} + \frac{\theta}{2} + c_0 \right]^{-1}.$$

For this mean-reverting dynamics, the interplay between risk (here solely due to the noise source variance σ^2) and the target band width $2\bar{f}$ on t_{relax} is opposite compared to the DMPS dynamics of section 2.

The tendency of the fundamental f to revert to its long-run level μ , for a narrow target band, generates an effect of an increase in risk (variance) that is opposite of the one generated by an increase of β in the DMPS setting, because of the latter's tendency to escape from the mean. If the band is larger, lower levels of σ initially increase the relaxation time, to ultimately achieving a decreasing effect. In both

cases, an increase in the size of the target band requires a higher T in order for the target zone to be credible.

We lastly notice that for the O-U case, zero is always the first eigenvalue (not surprising, given that it's an ergodic process) and a regime shift cannot be possible.

E Alternative to O-U dynamics: softly attractive drift

We now present the model where we model the fundamental as an ergodic process with a softly attractive drift instead of the Ornstein-Uhlenbeck dynamics. This framework has the advantage of incorporating mean-reverting dynamics while retaining analytical tractability. By “softly attractive” drift we mean the DMPS drift with opposite sign, i.e. $-\beta \tanh(\beta f)$. This model presents similar dynamics to the O-U framework, and allows for a stationary time-independent probability measure. The marginal difference with the O-U advantage is that the reversion of the fundamental to the mean is softer, and the advantage is that the full spectrum is available and the dynamics do not require an approximation. The equation for the exchange rate after applying Itô's lemma is now given by

$$\partial_t X(t, f) + \frac{1}{2} \partial_{ff} X(t, f) - \beta \tanh(\beta f) \partial_f X(t, f) - \frac{\alpha}{(1-r)} X(t, f) = -\frac{r\alpha}{(1-r)} f. \quad (28)$$

Using the equivalent transformation as in the DMPS case, we plug in Eq.(28) into Eq.(16) and obtain:

$$\begin{aligned} \int^f \cosh(\beta \zeta) \partial_t Y(t, \zeta) + \\ \frac{1}{2} [\beta \sinh(\beta f) Y(t, f) + \cosh(\beta f) \partial_f Y(t, f)] - \\ \beta \sinh(\beta f) Y(t, f) - \frac{\alpha}{(1-r)} \int^f \cosh(\beta \zeta) Y(t, \zeta) d\zeta = -\frac{r\alpha}{(1-r)} f. \end{aligned} \quad (29)$$

Now, taking once more the derivative of Eq.(29) with respect to f , one obtains:

$$\partial_t Y(t, f) + \frac{1}{2} \partial_{ff} Y(t, f) - \left[\frac{\beta^2}{2} + \frac{\alpha}{1-r} \right] Y(t, f) = -\frac{r\alpha}{(1-r)} \frac{f}{\cosh(\beta f)}. \quad (30)$$

Observe now that Eq.(30) is once again equivalent to the standard BM motion case and we can repeat the same procedure we . The spectrum will now include the eigenvalue zero since we deal with a stationary case.

We now proceed as before and Eq.(30) reads:

$$-\partial_\tau Y(\tau, f) + \frac{1}{2} \partial_{ff} Y(\tau, f) - \left[\frac{\beta^2}{2} + \frac{\alpha}{1-r} \right] Y(\tau, f) = -\frac{r\alpha}{(1-r)} \frac{f}{\cosh(\beta f)}. \quad (31)$$

Consider now the homogenous part of Eq.(31), namely:

$$-\partial_\tau Y(\tau, f) + \frac{1}{2} \partial_{ff} Y(\tau, f) - \left[\frac{\beta^2}{2} + \frac{\alpha}{1-r} \right] Y(\tau, f) = 0.$$

As done before, the method of separation of variables leads us to introduce $Y(\tau, f) = \phi(\tau)\psi(f)$ and the previous equation can be rewritten as:

$$\frac{-\partial_\tau \phi(\tau)}{\phi(\tau)} + \frac{1}{2} \frac{\partial_{ff} \psi(f)}{\psi(f)} - \left[\frac{\beta^2}{2} + \frac{\alpha}{1-r} \right] = 0.$$

and therefore we can write:

$$\begin{cases} \frac{-\partial_\tau \psi(\tau)}{\psi(\tau)} = \lambda_k, \\ \frac{1}{2} \frac{\partial_{ff} \psi(f)}{\psi(f)} - \left[\frac{\beta^2}{2} + \frac{\alpha}{1-r} \right] = \lambda_k \end{cases}$$

Defining $\Omega_k^2 = \left[\frac{\beta^2}{2} + \frac{\alpha}{1-r} \right] + \lambda_k$, the relevant eigenfunctions reads:

$$\psi(f) = c_1 \sin(\sqrt{2}\Omega_k f) + c_2 \cos(\sqrt{2}\Omega_k f).$$

Going back to Eq.(16), the boundary conditions at the borders of the target zone $\bar{f} = -\underline{f}$ reads:

$$\partial_f \left[\int^f \cosh(\beta\zeta) \psi(\zeta) d\zeta \right] \Big|_{f=\bar{f}} = 0.$$

which implies that:

$$\cosh(\beta\bar{f})\psi(\bar{f}) \quad \Rightarrow \quad c_1 = 0 \quad \text{and} \quad \Omega_k = (2k+1) \frac{\pi}{2\sqrt{2}\bar{f}}. \quad (32)$$

We note that Eq.(32) implies :

$$\lambda_k = \frac{(2k+1)^2 \pi^2}{8\bar{f}^2} - \frac{\beta^2}{2} - \frac{\alpha}{1-r} \geq 0. \quad (33)$$

Lastly, as expected, for the soft attractive case we are able to derive the exact spectrum analytically and unlike the DMPS case, there is no spectral gap.